arXiv:1612.07148v1 [hep-th] 21 Dec 2016

Algebraic Cutting Equations

Damiano Anselmi

Dipartimento di Fisica "Enrico Fermi", Università di Pisa,
Largo B. Pontecorvo 3, 56127 Pisa, Italy
and INFN, Sezione di Pisa,
Largo B. Pontecorvo 3, 56127 Pisa, Italy
damiano.anselmi@unipi.it

Abstract

We prove a set of polynomial identities for complex numbers associated with Feynman diagrams. The equations are at the core of perturbative unitarity in quantum field theory.

1 Introduction

Perturbative unitarity in quantum field theory is the statement that the scattering matrix S is unitary at the perturbative level. This property can be rephrased as a set of identities obeyed by the scattering amplitudes. At the diagrammatic level, it amounts to a set of *cutting equations*, which involve a diagram G together with the variants obtained by cutting G in various ways. In this paper, we show that perturbative unitarity can be conceptually reduced to a set of polynomial equations for complex numbers. We call such identities *algebraic cutting equations*. They are actually more general than what is strictly needed for the proof of perturbative unitarity, which is why we think that they deserve consideration on their own as mathematical properties.

The usual proof of perturbative unitarity [1, 2, 3] proceeds in four steps, which are the derivations of: (i) a diagrammatic equation in coordinate space known as *the largest time equation*, (ii) the cutting equations properly known (henceforth called *diagrammatic* cutting equations, to distinguish them from the algebraic ones), (iii) the pseudounitarity equation, and (iv) the unitarity equation $SS^\dagger = 1$. In this paper, we concentrate on a new, algebraic approach that allows us to jump directly to point (ii). We will not have much to say about the other steps just mentioned, which remain unmodified.

In particular, the projection $(iii) \to (iv)$ of the pseudounitarity equation onto the unitarity equation is necessary only in the presence of local symmetries. Its role is to show that the temporal and longitudinal components of the gauge fields are compensated by the Faddeev-Popov ghosts. The projection can be handled with the methods of refs. [2] and [3] in gauge theories and those of ref. [4] in gauge theories and gravity. The implication $(ii) \to (iii)$ is straightforward, since the pseudounitarity equation is just a collection of the cutting equations. The implication $(i) \to (ii)$ follows from the Fourier transform of the largest time equation plus the requirement that positive energies propagate forward in time and negative energies propagate backward in time. In the approach we offer here, it is a particular case of the general theorem we prove.

As of today, the step (i) is not optimized. The largest time equation is unnecessarily restrictive, while its common derivation is unnecessarily redundant. Being able to skip step (i) and get directly to point (ii) is economic in several respects, and allows us to gain a deeper understanding.

The polynomial identities we derive are associated with oriented Feynman diagrams and involve *polar* numbers. A polar number is a complex number to which a positive or negative polarity is assigned, the definition of polarity being arbitrary. The theorem states that certain polynomials of polar numbers are equal to sums of polarized monomials. A polar

monomial is a product of one polar number for each internal leg of the diagram. A polarized monomial is a polar monomial where at least one loop is polarized. A loop is polarized when each leg carries a polar number with a polarity that agrees with the leg orientation.

In the applications to physics, the legs of the diagrams are oriented according to energy flows. The polar numbers are "half propagators" and have a single pole (the propagator being the sum of two polar numbers). The polarity is positive or negative according to whether the pole is located below or above the real axis of the complex energy plane. The polarized monomials do not contribute to the diagrammatic cutting equations, because polarized loops give zero after the integration on the loop momentum. The polynomial identities thus lead to the diagrammatic cutting equations in a straightforward way.

We hope that the investigation of this paper contributes to make perturbative unitarity more familiar to readers, by uncovering its purely algebraic aspects and offering a clearer understanding and a more efficient control on its key aspects. As we show in section 8, the algebraic approach also helps organizing computations in more practical ways.

The paper is organized as follows. In section 2 we collect the basic definitions. In section 3 we state the main theorem, which we prove in section 4. In section 5 we collect a number of examples. Specifically, we use the algebraic identities to derive the diagrammatic cutting equations of the bubble and triangle diagrams at one loop and the chestnut diagram at two loops. We include the algebraic identities of other diagrams, up to three loops. In section 6 we use the identities to prove the perturbative unitarity of quantum field theories. In section 7 we discuss some symmetries of the algebraic cutting equations. Section 8 contains the conclusions, with emphasis on the virtues of the algebraic approach with respect to the usual approach.

2 Basic definitions

In this section we collect the basic definitions that are necessary to state the main theorem.

A diagram is a set of vertices connected by lines. The lines of a diagram will be called *legs* henceforth. The diagrams we consider do not need to be planar or connected. The vertices can be the endpoints of any number of legs, including one or two. The vertices that are attached to a unique leg are called external. The legs they are attached to are also called external. The other vertices and legs are called internal. From now on, we drop the external vertices and whenever we talk about vertices we mean the internal ones.

Equip the internal legs of the diagrams with orientations. The definition of oriented leg is self evident. Two legs are called adjacent if they have a vertex in common. Two adjacent legs are said to have coherent orientations if the orientation of one leg points to the vertex

in common and the orientation of the other leg points away from the vertex in common.

Definition 1 *Given a diagram, a curve is a sequence* $\{\ell_1, \dots \ell_n\}$ *of legs* ℓ_i*, such that each* ℓ_i *with* $i > 1$ *is adjacent to* ℓ_{i-1}*. A loop is a closed curve, i.e. a curve* $\{\ell_1, \dots \ell_n\}$ *such that* ℓ_1 *is adjacent to* ℓ_n*. A curve is minimal if it contains no loop. A loop is minimal if it contains no loop apart fom itself.*

An example of nonminimal loop is a loop that looks like an "8".

Definition 2 *A curve or a loop are oriented if the orientations of all their legs are coherent.*

Assume that G is connected and has I internal legs and V vertices. Pick I independent real numbers E_i, $i = 1, \dots I$, and call them "energies". Assign an energy to each internal leg and zero energy to each external leg. Use the orientation of a leg to define the orientation of the flow of its energy. Then, impose the energy conservation at each vertex. This is the requirement that the total energy flowing into the vertex must be equal to the total energy flowing out of the vertex. The independent conservation conditions are $V - 1$, because the total energies flowing into the diagram and out of it are zero by assumption. Due to this, the energy is automatically conserved in the last vertex, once it is conserved in every other vertex. Energy conservation leaves us with $I - V + 1 \equiv L$ arbitrary independent energies $e_1, \dots e_L$.

Proposition 1 *It is possible to arrange the leg orientations and the energies* $e_1, \dots e_L$*, so that the flow of each energy defines an oriented minimal loop in* G *and each leg is associated with a linear combination of energies* $e_1, \dots e_L$ *with coefficients 0 or 1.*

Proof. To see this, start from the diagram G, with no leg orientations and zero energy in every leg. Assume, for the time being, that G is one-particle irreducible. Consider a minimal loop γ_1 in G. Arrange the orientations of the γ_1 legs so that they are coherent and add the energy e_1 to each of its legs. So doing, the loop γ_1 becomes oriented. If $L = 1$, the construction stops here.

Otherwise, since G is one-particle irreducible, there must exist a pair $v^{(a)}$, $v^{(b)}$ of γ_1 vertices that are connected by a minimal curve Γ_{ab} which has no legs and no other vertex in common with γ_1. We distinguish two cases: $v^{(a)} \neq v^{(b)}$ and $v^{(a)} = v^{(b)}$. If $v^{(a)} \neq v^{(b)}$, $v^{(a)}$ and $v^{(a)}$ are connected both by Γ_{ab} and by two portions Δ_{ab} and Δ'_{ab} of γ_1. Pick the portion of your choice, say Δ_{ab}. The union $\Gamma_{ab} \cup \Delta_{ab}$ defines a minimal loop γ_2. The orientation of Δ_{ab} can be extended coherently to Γ_{ab}, to define the orientation of γ_2. Once this is done, add the energy e_2 to each leg of γ_2. If $v^{(a)} = v^{(b)}$, just pick Γ_{ab} as the loop γ_2 and orient it in the way you like. Then add e_2 to each of its legs. If $L = 2$, the construction stops here.

Observe that any distinct vertices $v^{(c)}$ and $v^{(d)}$ of $\gamma_1 \cup \gamma_2$ are connected by an oriented minimal curve Δ_{cd} contained in $\gamma_1 \cup \gamma_2$: if they both belong to γ_1 or γ_2, this fact is obvious. If $v^{(c)}$ belongs to γ_1 and $v^{(d)}$ belongs to γ_2, it is sufficient to move along γ_1 (following the γ_1 orientation) from $v^{(c)}$ to the first intersection between γ_1 and γ_2, then continue to $v^{(d)}$ along the portion of γ_2 that has a coherent orientation. Clearly, such a Δ_{cd} is a minimal curve.

If $L > 2$, there must exist a pair of vertices $v^{(c)}$ and $v^{(d)}$ of $\gamma_1 \cup \gamma_2$ that are connected by a minimal curve Γ_{cd} that has no legs and no other vertex in common with $\gamma_1 \cup \gamma_2$. If $v^{(c)} \neq v^{(d)}$, by the property shown above they are also connected by an oriented minimal curve Δ_{cd} contained in $\gamma_1 \cup \gamma_2$. The union $\Gamma_{cd} \cup \Delta_{cd}$ of the two curves defines the third minimal loop γ_3, which becomes oriented after the orientation of Δ_{ab} is coherently extended to the whole loop. Finally, the energy e_3 is added to all the legs of γ_3. If $v^{(c)} = v^{(d)}$, just pick Γ_{cd} as γ_3, orient it in the way you like and add e_3 to each of its legs. If $L = 3$, the construction stops here.

Again, any pair of distinct vertices that belong to the union $\gamma_1 \cup \gamma_2 \cup \gamma_3$ are connected by an oriented curve contained in $\gamma_1 \cup \gamma_2 \cup \gamma_3$, which we can choose to be minimal. This allows us to iterate the construction for $L > 2$.

It is also straightforward to extend the assignments to the one-particle reducible diagrams as well as the disconnected diagrams. This concludes the proof. □

Definition 3 *A diagram is oriented if its leg orientations are compatible with the construction of proposition 1. Otherwise, the diagram is jammed.*

We call $e_1, \dots e_L$ *loop energies*. A diagram may admit various orientations, which give equivalent polynomial identities.

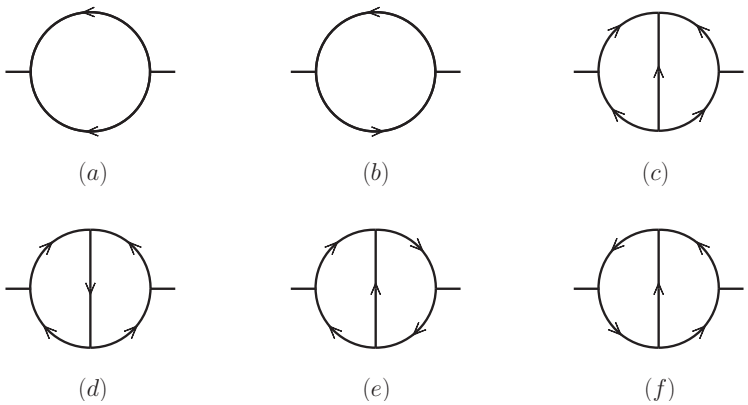

(2.1)

In this figure we show various examples. The diagrams (a) and (c) are jammed, while (b), (d), (e) and (f) are oriented. In particular, (d), (e) and (f) are different orientations of the same diagram. A diagram has precisely L oriented minimal loops. For example, (d), (e) and (f) have two oriented minimal loops.

3 The theorem

In this section we state the theorem, leaving its proof to the next section.

Let G denote an oriented diagram and $\ell_1, \dots \ell_I$ its internal legs. Let ν_a, $a = 1, \dots V$, label the vertices of the diagram. When we want to specify that the orientation of the ith leg points from, say, the vertex ν_a to the vertex ν_b, we denote it by $(\nu_a \ell_i \nu_b)$.

Build variants G_M of G by marking any number of vertices. We denote the marked vertices by $\hat{\nu}_a$. The marked diagrams have legs of types $(\nu_a \ell_i \hat{\nu}_b)$, $(\hat{\nu}_a \ell_i \nu_b)$ and $(\hat{\nu}_a \ell_i \hat{\nu}_b)$, besides those of type $(\nu_a \ell_i \nu_b)$, the leg orientation pointing from a to b.

Let $\{\sigma_i^+, \tau_i^+, \sigma_i^-, \tau_i^-\}$, $i = 1, \dots I$, denote I quartets of complex numbers, one quartet for each leg, arranged into pairs $\{\sigma_i^+, \tau_i^+\}$ and $\{\sigma_i^-, \tau_i^-\}$. We say that σ_i^+, τ_i^+ (σ_i^-, τ_i^-) have positive (negative) polarities and call them *polar numbers*.

Define the *propagators*

$$z_i = \sigma_i^+ + \sigma_i^-, \qquad w_i = \tau_i^+ + \tau_i^-, \qquad u_i = \sigma_i^+ + \tau_i^-, \qquad v_i = \sigma_i^- + \tau_i^+. \tag{3.1}$$

The *value* P_M of the diagram G_M is determined by the following "Feynman" rules. Assign the value one to each unmarked vertex and the value -1 to each marked one. Associate propagators with the legs of G_M as follows:

$$(\nu \ell_i \nu') \to z_i, \qquad (\hat{\nu} \ell_i \hat{\nu}') \to w_i, \qquad (\nu \ell_i \hat{\nu}') \to u_i, \qquad (\hat{\nu} \ell_i \nu') \to v_i. \tag{3.2}$$

Graphically, we denote the marked vertices by means of a dot, so the propagators are

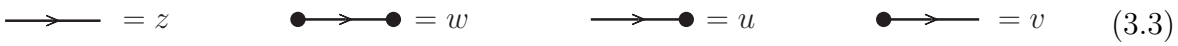

(3.3)

Then, P_M is the polynomial

$$P_M = (-1)^m \prod_{i=1}^{I} p_{Mi}, \tag{3.4}$$

where p_{Mi} denotes the propagator of the ith leg ℓ_i, assigned according to the scheme (3.2), and m is the number of marked vertices.

For example, the polynomials associated with the marked diagrams

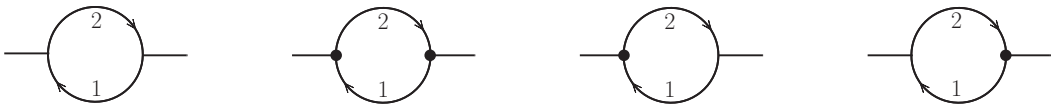

(3.5)

are

$$z_1 z_2, \qquad w_1 w_2, \qquad -u_1 v_2, \qquad -v_1 u_2, \tag{3.6}$$

respectively.

The set or marked diagrams includes the diagram G itself, where all the vertices are unmarked, as well as the diagram $\bar{G}$ where all the vertices are marked. The polynomials P and $\bar{P}$ associated with G and $\bar{G}$ are

$$P = \prod_{i=1}^{I} z_i, \qquad \bar{P} = (-1)^V \prod_{i=1}^{I} w_i,$$

respectively.

The theorem is about the sum of the polynomials P_M on all the ways M to mark the diagram G. Writing z, w, u and v as sums of polar numbers, according to formula (3.1), we can expand the sum of P_M as a sum of *polar monomials*. A polar monomial is the product of one polar number of the set $\{\sigma_i^+, \tau_i^+, \sigma_i^-, \tau_i^-\}$ for each leg ℓ_i. A polar curve, loop or diagram is a curve, loop or diagram whose legs are equipped with polar numbers.

Examples of polar monomials for the diagram G of equation (3.5) are

$$\sigma_1^+\sigma_2^+, \qquad \sigma_1^-\tau_2^-, \qquad \sigma_1^+\sigma_2^-, \qquad \sigma_1^+\tau_2^-, \qquad \sigma_1^-\tau_2^+, \tag{3.7}$$

etc.

Definition 4 *A polarized loop is a polar loop where adjacent legs of coherent (opposite) orientations carry polar numbers of coherent (opposite) polarities.*

In particular, an oriented polar loop is polarized if all its legs carry polar numbers of the same polarity. Instead, a polarized nonoriented loop is such that the leg polarity flips if and only if the orientation flips.

Definition 5 *A polarized monomial is a polar monomial where at least one loop is polarized.*

Consider, for example, the figures

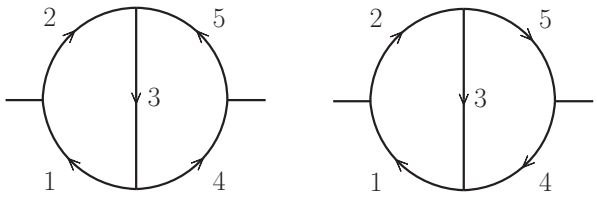

(3.8)

The oriented loops of the first diagram are 123 and 345, while 1254 is a non oriented loop. If we equip such loops with the polar monomials $\sigma_1^+\sigma_2^+\tau_3^+$, $\sigma_3^-\tau_4^-\tau_5^-$ and $\sigma_1^+\sigma_2^+\sigma_4^-\tau_5^-$, respectively, we obtain polarized loops. Examples of polarized monomials are $\sigma_1^+\sigma_2^+\tau_3^+\sigma_4^+\tau_5^-$ and $\sigma_1^+\sigma_2^+\sigma_3^-\tau_4^-\tau_5^-$. Examples of polarized loops for the second diagram of figure (3.8) are 123 with the monomial $\sigma_1^+\sigma_2^+\tau_3^+$, 1254 with $\sigma_1^+\sigma_2^+\tau_4^+\sigma_5^+$ and 345 with $\sigma_3^+\sigma_4^-\tau_5^-$.

Here is the main theorem of this paper:

Theorem 1 *given a diagram G, the identity*

$$\sum_{markings\ M} P_M = \mathcal{P}_G \tag{3.9}$$

holds, where $\mathcal{P}_G$ is a sum of polarized monomials.

We can condense the theorem by saying that the sum of the marked diagrams is equal to a sum of polarized diagrams.

For example, if we sum the polynomials (3.6), we can easily check the identity

$$z_1 z_2 + w_1 w_2 - u_1 v_2 - v_1 u_2 = (\sigma_1^+ - \tau_1^+)(\sigma_2^+ - \tau_2^+) + (\sigma_1^- - \tau_1^-)(\sigma_2^- - \tau_2^-). \tag{3.10}$$

Note that the right-hand side is a sum of polarized monomials. More examples are given in section 5.

At the tree level, we have $\mathcal{P}_G = 0$. At one loop, we have have the general formula

$$\mathcal{P}_G = \prod_{i=1}^{I} (\sigma_i^+ - \tau_i^+) + \prod_{i=1}^{I} (\sigma_i^- - \tau_i^-), \tag{3.11}$$

which we leave without proof, since it is not crucial for the rest of the discussion.

We can assume that the diagram G does not contain tadpoles, i.e. loops made of a single leg that begins and ends at the same vertex. Indeed, if G contains tadpoles, the theorem is trivial, since a tadpole is an oriented loop and can obviously be written as the sum of two contributions, each being a polar number, which is polarized by definition. Moreover, we can also assume that G is connected, since the theorem extends to disconnected diagrams in an obvious way, once it is proved for connected diagrams. Finally, we can assume $V > 1$, since a diagram with a single vertex has no internal leg (in which case the theorem is obvious) or is a tadpole.

4 Proof of the theorem

In this section we prove the theorem. Since formula (3.9) is a polynomial identity, if we prove it for polar numbers belonging to open sets of the complex plane, we automatically prove it for arbitrary polar numbers. Thus, with no loss of generality, we can assume that the signs of the imaginary parts of the polar numbers $\sigma_i^+, \tau_i^+, \sigma_i^-, \tau_i^-$ coincide with their polarities.

Let G denote an oriented connected diagram with I internal legs, V vertices, $L = I - V + 1$ loops and no tadpoles. Denote the internal legs by ℓ_i, $i = 1, \dots I$, and the vertices by ν_a, $a = 1, \dots V$. We can assume $V > 1$ and equip G with loop energies $e_1, \dots, e_L$ in the way specified by proposition 1.

If more external legs are attached to the same vertex, drop all of them but one. If no external leg is attached to a vertex, add one. So doing, each vertex is attached to one external leg and the diagram G becomes a figure like

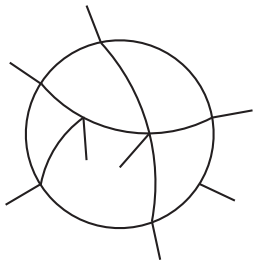

(4.1)

Note that some external legs are drawn inside the diagram, for no particular reason other than aesthetics. They could be prolonged at will by crossing over the internal legs, since Feynman diagrams need not be planar.

Assign propagators identically equal to one to the external legs. Then, equip each external leg but the last one with an independent energy $\mathcal{E}_a$, $a = 1, \dots V-1$, that flows into the diagram. By the conservation of energy, the external leg attached to the last vertex ν_V has energy $\sum_{a=1}^{V-1} \mathcal{E}_a$ flowing out of the diagram.

By the argument of section 2, if G is one-particle irreducible, each pair of vertices $\{\nu_a, \nu_V\}$, $a = 1, \dots V-1$, is connected by a minimal curve Γ_a in G that is oriented from ν_a to ν_V. This property can be easily extended to any connected diagram G. If G is one-particle reducible, it can be viewed as a sequence of one-particle irreducible subdiagrams G_A, $A = 1, \dots N$, and single (nonoriented) lines ℓ_A, $A = 1, \dots N-1$, connecting G_A to G_{A+1}. Equip ℓ_A with the orientation that flows towards the subdiagram $\tilde{G}_A$ that contains ν_V. Then, given a pair of vertices $\{\nu_a, \nu_V\}$, $a = 1, \dots V-1$, it is possible to connect them through a minimal curve Γ_a that is oriented from ν_a to ν_V and is equal to the union of a set of oriented minimal curves $\Gamma'_A \subset G_A$ and lines ℓ_A.

Add the energy $\mathcal{E}_a$ to all the legs of Γ_a. Let E_i denote the energy of the ith internal leg ℓ_i. By proposition 1 and the construction just described, E_i is a linear combination of the loop energies $e_1, \dots, e_L$ and the external energies $\mathcal{E}_1, \dots, \mathcal{E}_{V-1}$, with coefficients 0 or 1.

Define new polar numbers $\zeta_i^\pm$ and $\xi_i^\pm$ as

$$\zeta_i^\pm = E_i - (\sigma_i^\pm)^{-1}, \qquad \xi_i^\pm = E_i - (\tau_i^\pm)^{-1}. \tag{4.2}$$

Their polarities, specified by the superscripts $+$ and $-$, coincide with the signs of their imaginary parts. We have

$$\sigma_i^\pm(E_i) = \frac{1}{E_i - \zeta_i^\pm}, \qquad \tau_i^\pm(E_i) = \frac{1}{E_i - \xi_i^\pm}. \tag{4.3}$$

For a while, we keep $\zeta_i^\pm$ and $\xi_i^\pm$ fixed and treat $\sigma_i^\pm$ and $\tau_i^\pm$ as functions of the energies. In some intermediate steps we integrate over the loop energies. Then, we undo the integral to recover properties that hold at arbitrary energies. This is the strategy that leads to the proof of the theorem.

Now, pick a marked diagram G_M, take formula (3.4), implement the replacements (4.3) and integrate each loop energy e_j along the real axis with the measure $\mathrm{d}e_j/(2\pi)$. This defines the value of G_M in energy space, which is

$$G_M(\mathcal{E}_1, \dots, \mathcal{E}_{V-1}) = (-1)^m \int \prod_{i=1}^{I} p_{Mi}(E_i) \prod_{j=1}^{L} \frac{\mathrm{d}e_j}{2\pi}. \tag{4.4}$$

This integral is overall convergent, because it is well behaved at infinity and no pole sits on the real axis. As far as the overall behavior at infinity is concerned, observe that each polar number decreases like $1/e$, where e collectively denotes the loop energies, so the overall behavior of P_M is $1/e^I$, which falls off fast enough, since $V > 1$ implies $I = L+V-1 \geqslant L+1$. Moreover, every subintegral is overall convergent for a similar reason. Incidentally, the reason why we cannot treat diagrams that contain tadpoles is that they do not satisfy these conditions.

We move to the coordinate versions of the diagrams, by taking their Fourier transforms. The Fourier transforms of the polar numbers $\sigma_j^\pm$ and $\tau_j^\pm$ are

$$\tilde\sigma_j^\pm(t_j) = \int_{-\infty}^{+\infty} \frac{\mathrm{d}E_j}{2\pi} \frac{\mathrm{e}^{iE_jt_j}}{E_j - \zeta_j^\pm} = \pm i\theta(\pm t_j)\mathrm{e}^{it_j\zeta_j^\pm}, \qquad \tilde\tau_j^\pm(t_j) = \pm i\theta(\pm t_j)\mathrm{e}^{it_j\xi_j^\pm}.$$

Familiar knowledge of quantum field theory tells us that the coordinate version $\tilde G_M$ of (4.4) [multiplied by the distribution $(2\pi)\delta(\mathcal{E}_1 + \mathcal{E}_2 + \cdots + \mathcal{E}_V)$, which imposes the overall energy conservation, where $\mathcal{E}_V$ is an independent energy] is the product of the propagators in coordinate space, times the values of the vertices, integrated over the locations μ_a of the vertices, i.e.

$$\tilde G_M(t_1, \dots, t_V) = (-1)^m \int \prod_{a=1}^{V} [\mathrm{d}\mu_a \delta(t_a - \mu_a)] \prod_{j=1}^{I} \tilde p_{Mj}(\mu_{a_j} - \mu_{b_j}).$$

Here $\tilde p_{Mj}(\mu_{a_j} - \mu_{b_j})$ denotes the Fourier transform of the propagator p_{Mj} associated with the line ℓ_j and μ_{a_j}, μ_{b_j} are the time coordinates of the ℓ_j endpoints, ordered so that the ℓ_j orientation points from the vertex of time μ_{a_j} to the vertex of time μ_{b_j}. The delta functions are the Fourier transforms of the propagators of the external legs (which are identically one in energy space).

The μ integrals are straightforward, so we just get

$$\tilde{G}_M(t_1,\dots,t_V) = (-1)^m \prod_{j=1}^{I} \tilde{p}_{Mj}(t_{a_j} - t_{b_j}).$$

We can formulate the Feynman rules of the diagrams in coordinate space are as follows. As usual, the unmarked vertices are equal to one and the marked vertices are equal to -1. The propagators $\tilde{p}_{Mj}(t_a - t_b)$ are assigned according to the scheme

$$\begin{aligned}
&(\nu_a \ell_j \nu_b) \to z_j = \sigma_j^+ + \sigma_j^- \to i\theta(t_{ab}) \mathrm{e}^{it_{ab}\zeta_j^+} - i\theta(-t_{ab}) \mathrm{e}^{it_{ab}\zeta_j^-}, \\
&(\nu_a \ell_j \hat{\nu}_b) \to u_j = \sigma_j^+ + \tau_j^- \to i\theta(t_{ab}) \mathrm{e}^{it_{ab}\zeta_j^+} - i\theta(-t_{ab}) \mathrm{e}^{it_{ab}\xi_j^-}, \\
&(\hat{\nu}_a \ell_j \nu_b) \to v_j = \sigma_j^- + \tau_j^+ \to i\theta(t_{ab}) \mathrm{e}^{it_{ab}\xi_j^+} - i\theta(-t_{ab}) \mathrm{e}^{it_{ab}\zeta_j^-}, \\
&(\hat{\nu}_a \ell_j \hat{\nu}_b) \to w_j = \tau_j^+ + \tau_j^- \to i\theta(t_{ab}) \mathrm{e}^{it_{ab}\xi_j^+} - i\theta(-t_{ab}) \mathrm{e}^{it_{ab}\xi_j^-},
\end{aligned} \tag{4.5}$$

where $t = t_a - t_b$ and t_a denotes the time coordinate of the vertex ν_a.

Now we show that

Lemma 1 *the identity*

$$\sum_{markings\ M} \tilde{G}_M(t_1,\dots,t_V) = 0 \tag{4.6}$$

holds.

Proof. We can assume that the vertices have distinct times, because the distributions (4.5) and the left-hand side of (4.6) do not involve contact terms. Then, there is a lowest time, which we denote by t_0. Let $\varkappa$ denote its vertex. Formula (4.6) holds, because the sum on the left-hand side contains pairs of mutually canceling contributions,

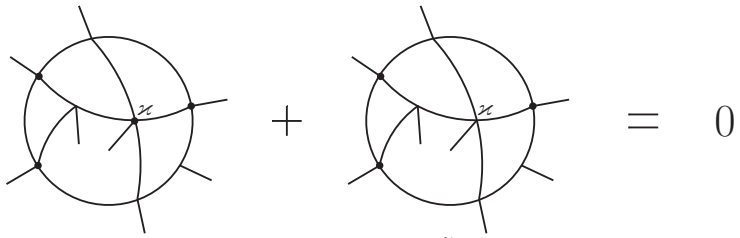

(4.7)

Specifically, for every diagram G_M that has $\varkappa$ unmarked, there is an almost identical diagram G'_M that differs from G_M just for the marking of $\varkappa$. The contribution $\tilde{G}'_M$ due to G'_M is opposite to the contribution $\tilde{G}_M$ due to G_M, because the extra marking implies an extra minus sign. On the other hand, all the propagators of G_M and G'_M have equal values. Those

that do not involve $\varkappa$ coincide, because they connect the same vertices. Those that involve $\varkappa$ coincide, because the scheme (4.5) implies

$$\begin{aligned}
&(\varkappa\ell_j\nu_b) \to -i\mathrm{e}^{i(t_0-t_b)\zeta_j^-}, \qquad &&(\varkappa\ell_j\hat\nu_b) \to -i\mathrm{e}^{i(t_0-t_b)\xi_j^-},\\
&(\hat\varkappa\ell_j\nu_b) \to -i\mathrm{e}^{i(t_0-t_b)\zeta_j^-}, \qquad &&(\hat\varkappa\ell_j\hat\nu_b) \to -i\mathrm{e}^{i(t_0-t_b)\xi_j^-},\\
&(\nu_a\ell_j\varkappa) \to i\mathrm{e}^{i(t_a-t_0)\zeta_j^+}, \qquad &&(\hat\nu_a\ell_j\varkappa) \to i\mathrm{e}^{i(t_a-t_0)\xi_j^+},\\
&(\nu_a\ell_j\hat\varkappa) \to i\mathrm{e}^{i(t_a-t_0)\zeta_j^+}, \qquad &&(\hat\nu_a\ell_j\hat\varkappa) \to i\mathrm{e}^{i(t_a-t_0)\xi_j^+},
\end{aligned}$$

which shows that in all cases a marked $\varkappa$ gives the same propagator as does an unmarked $\varkappa$. □

The next step is to extract useful pieces of information from the result (4.6). The left-hand side of equation (3.9) can be expanded as a sum

$$\sum_{\text{markings } M} (-1)^m \prod_{i=1}^{I} p_{Mi}(E_i) = \sum_\theta c_\theta \prod\nolimits_{i=1}^{I} \frac{1}{E_i-\theta_i} \tag{4.8}$$

of polar monomials

$$\prod\nolimits_{i=1}^{I} \frac{1}{E_i-\theta_i}, \tag{4.9}$$

where θ is an assignment of polar numbers $\theta_i = \zeta_i^+$, ξ_i^+, ζ_i^- or ξ_i^- to the legs ℓ_i of the diagram and c_θ are numerical coefficients. When we integrate on the loop energies,

$$\sum_\theta c_\theta \int \prod\nolimits_{i=1}^{I} \frac{1}{E_i-\theta_i} \prod\nolimits_{j=1}^{L} \frac{\mathrm{d}e_j}{2\pi}, \tag{4.10}$$

multiply by $(2\pi)\delta(\sum_{i=1}^{V}\mathcal{E}_i)$ and take the Fourier transform, we get the left-hand side of (4.6). If we make these operations on a single polar monomial (4.9), we obtain a contribution that is proportional to a product of θ functions times various exponential factors. We schematically write it as

$$\prod\nolimits_{j=1}^{I} \theta(\Delta t_j)\mathrm{e}^{i\rho_j\Delta t_j} = \Theta(t_1,\dots,t_I)\prod\nolimits_{j=1}^{I}\mathrm{e}^{i\rho_j\Delta t_j}, \qquad \text{where} \quad \Theta(t_1,\dots,t_I) \equiv \prod\nolimits_{j=1}^{I}\theta(\Delta t_j). \tag{4.11}$$

Here ρ_j can be ζ_j^+, ξ_j^+, $-\zeta_j^-$ or $-\xi_j^-$, and $\Delta t_j = t_{a_j} - t_{b_j}$ in the first two cases, $\Delta t_j = t_{b_j} - t_{a_j}$ in the other two. Note that each product of exponential factors is associated with a unique distribution $\Theta(t_1,\dots,t_I)$.

We start from the knowledge that the left-hand side of (4.6) vanishes. We can isolate each contribution (4.11) from the others by looking at the exponential factors. Since the numbers ζ_j^+, ξ_j^+, ζ_j^- and ξ_j^- can be chosen arbitrarily, apart from the signs of their imaginary parts, each contribution (4.11) must disappear independently from equation (4.6).

The Fourier transform (4.11) of a polar monomial can disappear from (4.6) for two reasons: the numerical coefficient c_θ in front of it vanishes, or the distribution $\Theta(t_1, \dots, t_I)$ is identically equal to zero. Consequently, the right-hand side of (3.9) can only contain the polar monomials that have a vanishing $\Theta(t_1, \dots, t_I)$. Thus, it is mandatory to understand when that happens.

Consider the distribution $\Theta(t_1, \dots, t_I)$ together with the "naked" diagram G, that is to say the diagram G with no markings on the vertices and no orientations on the lines. We want to use $\Theta(t_1, \dots, t_I)$ to equip G with a *time ordering*, which has nothing to do with the orientation based on the energy flow met so far. Precisely, we equip each G internal line with an arrow pointing from the endpoint of lower time to the endpoint of larger time. Denote the diagram obtained this way by $G_{\rm or}$,

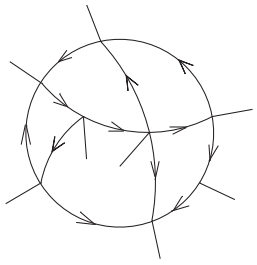

$G_{\rm or}$ (4.12)

and its distribution $\Theta(t_1, \dots, t_I)$ by $\Theta(G_{\rm or})$.

We say that a curve γ is time ordered if its lines have coherent time orientations. We denote the product of the theta functions associated with its lines by $\Theta(\gamma)$.

If γ is not time ordered and t_a, t_b are the times associated with its endpoints, $\Theta(\gamma)$ is nontrivial both for $t_a > t_b$ and $t_a < t_b$. To see this, observe that, since we are just interested in the endpoints, two adjacent lines with coherent time orderings can be collapsed onto a single line with the same ordering. Thus, it is sufficient to consider the cases

(4.13)

etc., where time is the vertical coordinate. It is evident that for arbitrary t_a and t_b, there exist configurations of the intermediate vertices that make $\Theta(\gamma)$ nontrivial.

Now we prove two useful lemmas. The first one is a generalization of the property just shown.

Lemma 2 *Let ν_a and ν_b denote two distinct vertices of G_{or}. Denote their times by t_a and t_b, respectively. Assume that $\Theta(G_{or})$ is nontrivial, but vanishes identically for $t_a > t_b$. Then G_{or} contains a time ordered curve that connects ν_a to ν_b.*

Proof. The distribution $\Theta(G_{\rm or})$ can be viewed as a set constraints on the relative times of the nearest neighbors. When any of those constraints is violated, $\Theta(G_{\rm or})$ vanishes. Assume that $\Theta(G_{\rm or})$ forces a vertex ν, different from ν_a and ν_b, to be in the future of all its nearest neighbors. If so, send ν to the infinite future, which is equivalent to dropping ν and cutting the legs attached to it. Similarly, if $\Theta(G_{\rm or})$ forces a vertex $\bar\nu \neq \nu_a, \nu_b$ to be in the past of all its nearest neighbors, send it to the infinite past. Once both types of vertices are dropped, a reduced diagram $G'_{\rm or}$ is obtained, equipped with a reduced distribution $\Theta(G'_{\rm or})$. Since $\Theta(G_{\rm or})$ vanishes identically for $t_a > t_b$, $\Theta(G'_{\rm or})$ satisfies the same property. Next, repeat the procedure on $G'_{\rm or}$: $\Theta(G'_{\rm or})$ may force other vertices, different from ν_a and ν_b, to be in the past or future of all their nearest neighbors; if we drop them, we obtain a further reduced diagram $G''_{\rm or}$, on which we can iterate again. At the end, we remain with a reduced diagram $G^{\rm red}_{\rm or}$ that contains ν_a, ν_b and possibly vertices that are forced to have both past and future nearest neighbors. Moreover, $\Theta(G^{\rm red}_{\rm or})$ vanishes identically for $t_a > t_b$. In particular, $G^{\rm red}_{\rm or}$ cannot contain just ν_a and ν_b, because in that case the distribution $\Theta(G^{\rm red}_{\rm or})$ would be identically one. We infer that $G^{\rm red}_{\rm or}$ must contain at least one vertex ν besides ν_a and ν_b. Then, ν must have a future neighbor $\nu_{\rm f}$ and a past neighbor $\nu_{\rm p}$. Similarly, $\nu_{\rm f}$ must have a future neighbor $\nu'_{\rm f}$, while $\nu_{\rm p}$ must have a past neighbor $\nu'_{\rm p}$. Continuing like this, we eventually reach ν_b in the future and ν_a in the past, and identify a time ordered curve γ_{ab} that connects ν_a to ν_b. □

Lemma 3 *The distribution $\Theta(G_{or})$ is trivial if and only if G_{or} contains a time ordered loop.*

For example, the diagram of figure (4.12) has a time ordered loop. A time ordered loop clearly vanishes, because the theta functions conflict with one another, as in

$$\theta(t_1 - t_2)\theta(t_2 - t_1), \qquad \theta(t_1 - t_2)\theta(t_2 - t_3)\theta(t_3 - t_1). \tag{4.14}$$

The key content of the Lemma is that this is the only situation that can make $\Theta(t_1, \ldots, t_I)$ vanish.

Proof. Assume that $G_{\rm or}$ is a tree diagram. Then, the distribution $\Theta(G_{\rm or})$ is nontrivial, because it just orders the vertices according to time: the configurations $t_1, \ldots, t_I$ where $\Theta(t_1, \ldots, t_I)$ is equal to one have nonvanishing measure.

Now, proceed by induction. Assume that the theorem holds for diagrams with L loops or less. Consider an $(L+1)$-loop diagram $G_{\rm or}$. Cut one leg $(\nu_a \bar\ell \nu_b)$, so as to obtain an L loop

diagram G_L, which satisfies the theorem by the inductive assumption. If $\Theta(G_L)$ is trivial, it has a time oriented loop and so does $\Theta(G_{\rm or})$. If $\Theta(G_L)$ is nontrivial, we distinguish two cases: (i) $\Theta(G_L)$ is nontrivial for both $t_a < t_b$ and $t_a > t_b$; (ii) $\Theta(G_L)$ is trivial for either $t_a < t_b$ or $t_a > t_b$. When we close the $(L+1)$-th loop, the leg $(\nu_a \bar{\ell} \nu_b)$ orders the times t_a and t_b. In case (i), $\Theta(G_{\rm or})$ is nontrivial. In case (ii), $\Theta(G_{\rm or})$ is trivial if and only if the time ordering due to $(\nu_a \bar{\ell} \nu_b)$ conflicts with the one due to $\Theta(G_L)$. By Lemma 2, G_L contains a time ordered curve γ_{ab} connecting ν_a and ν_b. Thus, $\Theta(G_{\rm or})$ is trivial if and only if the union of $(\nu_a \bar{\ell} \nu_b)$ and γ_{ab} is a time oriented loop. $\square$

Now, let us go back to equation (4.8), that is to say the expansion of the left-hand side of (3.9) in terms of polar monomials (4.9). We recall that every polar monomial leads to a contribution (4.11), when we integrate on the loop energies and take the Fourier transform. Since each contribution (4.11) is independent of the others, equation (4.6) implies that every time the distribution $\Theta(t_1, \dots, t_I)$ is nontrivial, the coefficient c_θ must vanish. Thus, the right-hand side of (4.8) contains only the polar monomials (4.9) that lead to a trivial $\Theta(t_1, \dots, t_I)$. Moreover, we have just proved that $\Theta(t_1, \dots, t_I)$ is trivial if and only if $G_{\rm or}$ contains a time ordered loop $\gamma_{\rm or}$, i.e. $\Theta(\gamma_{\rm or})$ is trivial. Now we have to understand how this requirement reflects on the polar monomial (4.9).

Consider the legs ℓ_i of $\gamma_{\rm or}$ and collect the values of their indices i into the set $s_{\rm or}$. Multiply $\Theta(\gamma_{\rm or})$ by the appropriate exponential factors $\mathrm{e}^{i\rho_j \Delta t_j}$, as in (4.11),

$$\Theta(\gamma_{\rm or}) \prod\nolimits_{j \in s_{\rm or}} \mathrm{e}^{i\rho_j \Delta t_j} = \prod\nolimits_{j \in s_{\rm or}} \theta(\Delta t_j) \mathrm{e}^{i\rho_j \Delta t_j}. \tag{4.15}$$

We first assume that $\gamma_{\rm or}$ is also oriented, in the sense of the energy flow. Then, the triviality of the distribution (4.15) leads, after Fourier transform, to the identity

$$\int_{-\infty}^{+\infty} \frac{\mathrm{d}e}{2\pi} \prod\nolimits_{i \in s_{\rm or}} \frac{1}{E_i - \theta_i} = 0, \tag{4.16}$$

for arbitrary values of ζ_i^+, ζ_i^-, ξ_i^+ and ξ_i^-, $i \in s_{\rm or}$, where e is the loop energy of $\gamma_{\rm or}$. Here, e is one of the loop energies $e_1, \dots, e_L$ and appears inside each E_i of (4.16) with coefficient $+1$.

Now we show that the identity (4.16) holds if and only if the polar numbers θ_i are all placed on the same side with respect to the real axis, which means that the loop $\gamma_{\rm or}$ is polarized. It is obvious that this condition is sufficient, because if we close the integration path on the half plane with no poles, the residue theorem gives zero. The condition is also necessary, as we show by reductio ad absurdum. Assume that the integral of (4.16) is identically zero when one or more poles are above the real axis and one or more poles are

below it. Move all the poles with positive imaginary parts into a single pole θ^+ and all those with negative imaginary parts into a single pole θ^-. This gives an integral of the form

$$\int_{-\infty}^{+\infty} \frac{1}{(e-\theta^+)^{n_+}(e-\theta^-)^{n_-}} \frac{\mathrm{d}e}{2\pi} = \binom{n_+ + n_- - 2}{n_+ - 1} \frac{i(-1)^{n_++1}}{(\theta^+ - \theta^-)^{n_++n_--1}},$$

which is obviously nonvanishing, contradicting the assumption. Thus, $\gamma_{\rm or}$ is polarized.

If $\gamma_{\rm or}$ is not oriented in the sense of the energy flow, its loop energy e must be defined anew, since it is not one of the standard integrations variables $e_1, \ldots, e_L$ we have been using so far. Choose a direction for the e flow along $\gamma_{\rm or}$ and split the set $s_{\rm or}$ into $s'_{\rm or} \cup s''_{\rm or}$, such that the legs ℓ_i with $i \in s'_{\rm or}$ have orientations coherent with the e flow, while the legs ℓ_i with $i \in s''_{\rm or}$ have orientations opposite to the e flow. Consider the integrand of (4.16) and write $E_i = e + E'_i$ for $i \in s'_{\rm or}$, $E_i = -e + E'_i$ for $i \in s''_{\rm or}$, where E'_i are energies independent of e. Then, the condition that the Fourier transform of (4.15) vanishes identically gives

$$\int_{-\infty}^{+\infty} \frac{\mathrm{d}e}{2\pi} \prod\nolimits_{i\in s'_{\rm or}} \frac{1}{E'_i + e - \theta_i} \prod\nolimits_{j\in s''_{\rm or}} \frac{1}{E'_j - e - \theta_j} = 0.$$

We know that this condition holds if and only if the poles are located on the same side of the complex plane with respect to the real e axis. This means that each θ_i with $i \in s'_{\rm or}$ must be located on one half plane and each θ_i with $i \in s''_{\rm or}$ must be located on the other half plane. We see again that the loop $\gamma_{\rm or}$ is polarized, i.e. adjacent $\gamma_{\rm or}$ legs of coherent (opposite) orientations carry polar numbers of coherent (opposite) polarities.

Since the conclusions hold for arbitrary energies, as well as arbitrary polar numbers ζ_i^+, ξ_i^+, ζ_i^- and ξ_i^-, it also holds for arbitrary polar numbers σ_i^+, τ_i^+, σ_i^- and τ_i^-. This gives formula (3.9) and concludes the proof. □

5 Examples and applications

In quantum field theory, we can decompose each propagator into the sum of two polar numbers, called "half propagators", each of which has a unique pole. The polarity refers to the location of the pole with respect to the real axis. From now on, positive (negative) polarity means that the pole is located below (above) the real axis.

A polarized monomial contains a polarized loop. As explained above, the integral on the energy of a polarized loop is equal to zero, because all the poles of its integrand are located on the same side with respect to the real axis. Therefore, the integral of the left-hand side of (3.9) on the loop momenta vanishes. This operation gives the diagrammatic cutting equation associated with the diagram G.

In this section, we illustrate these properties in various one-loop and two-loop diagrams and include the algebraic identities of other diagrams, up to three loops. In section 6 we generalize them to prove the perturbative unitarity of quantum field theories.

5.1 Bubble diagram

The "bubble" diagram is the diagram (b) of equation (2.1). Its marked versions are listed in equation (3.5) and lead to the polynomial identity (3.10). Now we show how to apply this identity and derive the diagrammatic cutting equations.

The value of the bubble diagram is given by the convolution of two propagators. In D dimensional scalar field theories, we have

$$\mathcal{B} = \int \frac{\mathrm{d}^D k}{(2\pi)^D} \frac{1}{k^2 - m_1^2 + i\epsilon} \frac{1}{(k-p)^2 - m_2^2 + i\epsilon'}. \tag{5.1}$$

For convenience, we keep the infinitesimal widths ϵ and ϵ' different from each other. The reason will become apparent below. The arguments that follow focus on the energy integral, which is convergent. We do not need to pay attention to the integral on the space momentum. That integral may diverge in certain dimensions D, in which case it can be defined by means of a regularization (the dimensional technique being the most convenient choice).

Define the polar numbers

$$\sigma_1^{\pm} = \pm \frac{1}{2\omega_{1\epsilon}} \frac{1}{k^0 \mp \omega_{1\epsilon}}, \qquad \sigma_2^{\pm} = \pm \frac{1}{2\omega_{2\epsilon'}} \frac{1}{k^0 - p^0 \mp \omega_{2\epsilon'}}, \qquad \tau_i^{\pm} = -(\sigma_i^{\mp})^*, \tag{5.2}$$

where the complex frequencies are $\omega_{1\epsilon} = \sqrt{\mathbf{k}^2 + m_1^2 - i\epsilon}$, $\omega_{2\epsilon'} = \sqrt{(\mathbf{k}-\mathbf{p})^2 + m_2^2 - i\epsilon'}$ and contain the ϵ, ϵ' prescriptions. We see that σ_i^+ and τ_i^+ have poles located below the real axis, while σ_i^- and τ_i^- have poles located above the real axis.

Note that the definition of polarity we use here differs from the one used in the proof of the previous section in several respects. In particular, the signs of the imaginary parts of $\sigma_i^{\pm}$ and $\tau_i^{\pm}$ do not agree with the signs of the imaginary parts of their poles. We recall that the algebraic theorem of section 3 works with any definition of polarity.

The combinations

$$z_1 = \sigma_1^+ + \sigma_1^- = \frac{1}{k^2 - m_1^2 + i\epsilon}, \qquad z_2 = \sigma_2^+ + \sigma_2^- = \frac{1}{(k-p)^2 - m_2^2 + i\epsilon'}, \qquad w_i = -z_i^*, \tag{5.3}$$

give the propagators and (minus) their conjugates.

Now, define the "cut propagators" u_i and v_i as

$$u_i = \sigma_i^+ + \tau_i^-, \qquad v_i = \sigma_i^- + \tau_i^+. \tag{5.4}$$

We call these combinations cut propagators even if they are defined at $\epsilon, \epsilon' \neq 0$. Strictly speaking, the usual cut propagators are obtained in the limits $\epsilon, \epsilon' \to 0$. For example, using $\omega_{1\epsilon} \sim \omega_1 - i\epsilon/(2\omega_1)$, where $\omega_1 = \omega_{1\epsilon}|_{\epsilon=0}$, we get

$$\lim_{\epsilon\to 0} u_1 = -2i\pi\theta(k^0)\delta(k^2 - m_1^2), \qquad \lim_{\epsilon\to 0} v_1 = -2i\pi\theta(-k^0)\delta(k^2 - m_1^2), \tag{5.5}$$

which are the usual cut propagators of a scalar field, multiplied by $-i$. The limits of u_2 and v_2 for $\epsilon' \to 0$ give (5.5) with the replacements $k \to k - p$ and $m_1 \to m_2$.

At this point, we can write the bubble diagram (5.1) and its conjugate in the form

$$\mathcal{B} = \int z_1 z_2, \qquad \mathcal{B}^* = \int w_1 w_2,$$

and use the polynomial identity (3.10). The decomposition (3.10) is advantageous for the integration over the loop energy k^0. Expand the right-hand side of (3.10) as a sum of polarized monomials and pick one such monomial at a time. Its poles are located on the same side of the complex plane with respect to the real axis. When we integrate k^0 along the real axis, we can close the integration path at infinity on the side that contains no poles. By the residue theorem, each polarized monomial gives zero. Thus, the momentum integral of the left-hand side of (3.10) also vanishes. This gives the relation

$$\mathcal{B} + \mathcal{B}^* = \int u_1 v_2 + \int v_1 u_2, \tag{5.6}$$

which graphically reads

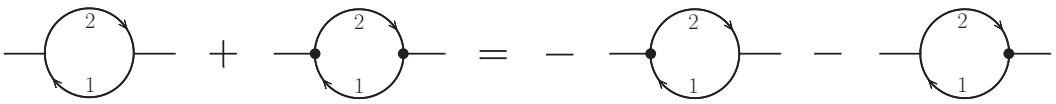

(5.7)

The Feynman rules are those of formula (3.3) (together with a factor -1 for every marked vertex).

The right-hand side of (5.7) is minus the sum of the cut diagrams, which is popularly represented as

(5.8)

by shadowing the areas that contain the marked vertices.

Note that ϵ, ϵ' are still different from zero, so the identity (5.6) is actually more general than the ones we are accustomed to in quantum field theory. Indeed, in those identities, the

cut propagators u_i are replaced by their limits (5.5). In our identity, instead, ϵ and ϵ' can be arbitrary positive numbers.

We see that the diagrammatic cutting equation (5.7) is a straightforward consequence of the simple polynomial identity (3.10).

5.2 Triangle and box diagrams

The "triangle" diagram is the one-loop oriented diagram with three adjacent lines. It leads to the polynomial identity

$$\begin{aligned} &z_1z_2z_3 - w_1w_2w_3 - u_1v_2z_3 - z_1u_2v_3 - v_1z_2u_3 + v_1u_2w_3 + w_1v_2u_3 + u_1w_2v_3 \\ &\qquad = \prod\nolimits_{i=1}^{3}(\sigma_i^+ - \tau_i^+) + \prod\nolimits_{i=1}^{3}(\sigma_i^- - \tau_i^-), \end{aligned} \tag{5.9}$$

which is easy to verify directly. The left-hand side of this formula can be worked out from the sum

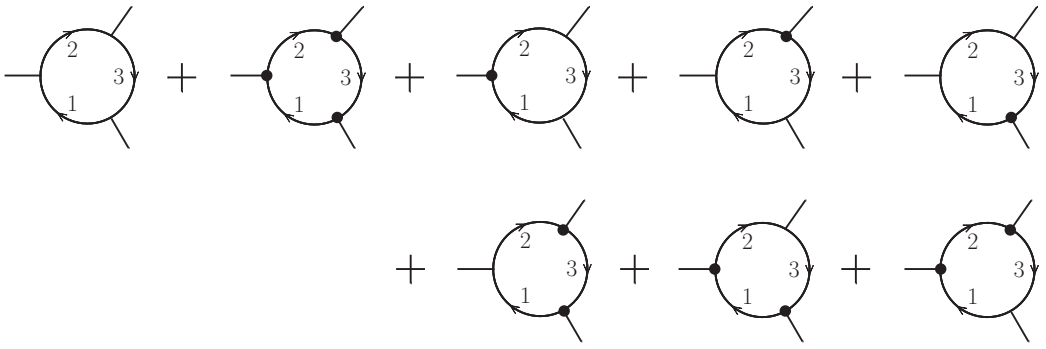

(5.10)

of the triangle diagram plus its marked versions, by applying the Feynman rules (3.3) and multiplying by $(-1)^m$, where m is the number of marked vertices. The right-hand side of (5.9) corresponds of the polynomial $\mathcal{P}_G$ of formula (3.9), which in the one-loop case is known in closed form due to formula (3.11).

The triangle diagram gives the integral

$$\mathcal{T} = \int \frac{\mathrm{d}^D k}{(2\pi)^D} \frac{1}{k^2 - m_1^2 + i\epsilon} \frac{1}{(k-p)^2 - m_2^2 + i\epsilon'} \frac{1}{(k-q)^2 - m_3^2 + i\epsilon''}, \tag{5.11}$$

where p and q are external momenta. To extend the analysis of the previous section, we add the definitions

$$\begin{aligned} &\sigma_3^\pm = \pm \frac{1}{2\omega_{3\epsilon''}} \frac{1}{k^0 - q^0 \mp \omega_{3\epsilon''}}, \qquad z_3 = \sigma_3^+ + \sigma_3^-, \qquad \tau_3^\pm = -(\sigma_3^\mp)^*, \qquad w_3 = -z_3^*, \\ &u_3 = \sigma_3^+ + \tau_3^-, \qquad v_3 = \sigma_3^- + \tau_3^+, \end{aligned} \tag{5.12}$$

to the previous ones, where $\omega_{3\epsilon''} = \sqrt{(\mathbf{k}-\mathbf{q})^2 + m_3^2 - i\epsilon''}$.

Again, we integrate both members of equation (5.9) on k^0. The right-hand side gives zero by the residue theorem, because of our definition of polarity, while the left-hand side leads to the identity

$$\mathcal{T} + \mathcal{T}^* - \int u_1 v_2 z_3 - \int z_1 u_2 v_3 - \int v_1 z_2 u_3 + \int v_1 u_2 w_3 + \int w_1 v_2 u_3 + \int u_1 w_2 v_3 = 0.$$

This formula is graphically represented by equating the sum (5.10) to zero. It can also be viewed as a diagrammatic cutting equation, by shadowing the marked areas of the diagrams. Once again, the diagrammatic cutting equation is rooted into the simple polynomial identity (5.9).

Without giving further details, we report the polynomial identity associated with the box diagram, which is

$$\begin{aligned} &z_1 z_2 z_3 z_4 + w_1 w_2 w_3 w_4 - u_1 v_2 z_3 z_4 + u_1 w_2 v_3 z_4 - u_1 w_2 w_3 v_4 - z_1 u_2 v_3 z_4 + z_1 u_2 w_3 v_4 - v_1 u_2 w_3 w_4 \\ &-z_1 z_2 u_3 v_4 + v_1 z_2 u_3 w_4 - w_1 v_2 u_3 w_4 - v_1 z_2 z_3 u_4 + w_1 v_2 z_3 u_4 - w_1 w_2 v_3 u_4 + v_1 u_2 v_3 u_4 + u_1 v_2 u_3 v_4 \\ &\quad = \prod_{i=1}^4 (\sigma_i^+ - \tau_i^+) + \prod_{i=1}^4 (\sigma_i^- - \tau_i^-). \end{aligned}$$

5.3 Two-loop and three-loop diagrams

Now we give a two-loop example, the chestnut diagram shown as first in the sum

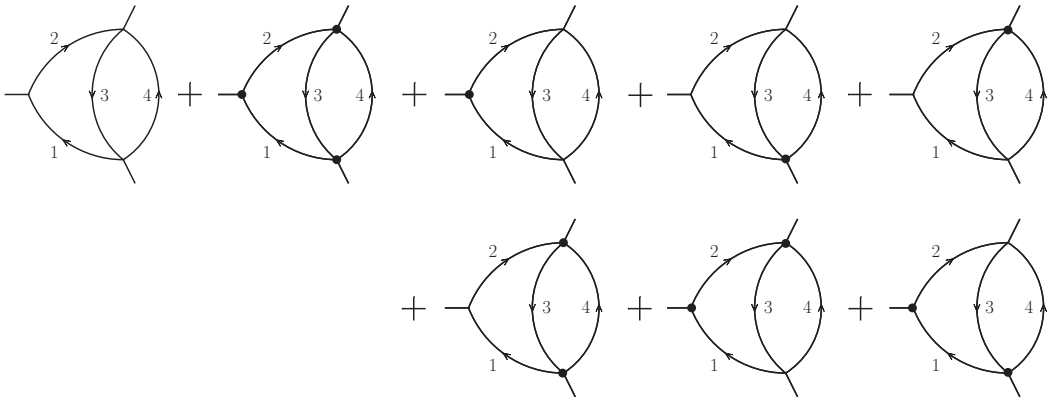

(5.13)

which includes its marked versions. The associated polynomial identity reads

$$\begin{aligned} &z_1 z_2 z_3 z_4 - w_1 w_2 w_3 w_4 - u_1 v_2 z_3 z_4 - v_1 z_2 u_3 v_4 - z_1 u_2 v_3 u_4 + v_1 u_2 w_3 w_4 + u_1 w_2 v_3 u_4 + w_1 v_2 u_3 v_4 \\ &\qquad = \sum \left[a \rho_1^+ \rho_2^+ \rho_3^+ \eta_4 + b \rho_1^- \rho_2^- \rho_3^- \eta_4 + c \eta_1 \eta_2 \rho_3^+ \rho_4^+ + d \eta_1 \eta_2 \rho_3^- \rho_4^- \right], \end{aligned} \quad (5.14)$$

where each ρ_i can stand for σ_i or τ_i and each η_i can stand for σ_i^+, σ_i^-, τ_i^+ or τ_i^-. The sum is over all such choices, a, b, c, d denoting unspecified numerical coefficients.

The oriented loops are 123 and 34. The loop 124 is redundant, because whenever it is polarized, either 123 or 34 is also polarized. The right-hand side of (5.14) is a sum of polarized monomials that factorize the polarized loops $\rho_1^+\rho_2^+\rho_3^+$, $\rho_1^-\rho_2^-\rho_3^-$, $\rho_3^+\rho_4^+$ or $\rho_3^-\rho_4^-$, as required by formula (3.9).

The chestnut diagram gives the loop integral

$$\mathcal{C} = \int \mathrm{d}\mu \frac{1}{k^2 - m_1^2 + i\epsilon_1} \frac{1}{(k-p)^2 - m_2^2 + i\epsilon_2} \frac{1}{(k+q-p')^2 - m_3^2 + i\epsilon_3} \frac{1}{q^2 - m_4^2 + i\epsilon_4},$$

where p and p' are external momenta and the measure $\mathrm{d}\mu$ is $\mathrm{d}^D k \mathrm{d}^D q/(2\pi)^{2D}$. The definitions of polar numbers, propagators and cut propagators are straightforward, mimicking the formulas (5.2), (5.3), (5.4) and (5.12). When we integrate on the loop momenta, the right-hand side of (5.14) gives zero, since every term contains a polarized oriented loop. The integral on the energy of that loop vanishes by the residue theorem, since the integrand has poles only above or below the real axis. In the end, we obtain the diagrammatic cutting equation graphically represented by equating the sum (5.13) to zero.

If we flip the orientations of the legs 3 and 4, we obtain a different orientation, for the diagram, and a different polynomial identity, which is equal to (5.14) upon exchange of the subscripts 3 and 4. In that case, the oriented loops become 124 and 34, so the right-hand side of (5.14) contains the polarized factors $\rho_1^+\rho_2^+\rho_4^+$, $\rho_1^-\rho_2^-\rho_4^-$, $\rho_3^+\rho_4^+$ and $\rho_3^-\rho_4^-$. The two orientations lead to equivalent identities for the integral $\mathcal{C}$, because they amount to send the loop momentum q to $-k-q$. To better see this, it is convenient to switch off the external momenta p and p', because they are not important for the polynomial identity.

We also report the polynomial identities associated with the two-loop self-energy diagrams of figure (3.8). The first diagram gives

$$\begin{aligned}
&z_1z_2z_3z_4z_5 + w_1w_2w_3w_4w_5 - u_1v_2z_3z_4z_5 - z_1u_2v_3z_4u_5 - z_1z_2z_3u_4v_5 - v_1z_2u_3v_4z_5 \\
&+u_1w_2v_3z_4u_5 + u_1v_2z_3u_4v_5 + w_1v_2u_3v_4z_5 + v_1u_2w_3v_4u_5 + z_1u_2v_3u_4w_5 + v_1z_2u_3w_4v_5 \\
&-v_1u_2w_3w_4w_5 - w_1v_2u_3w_4v_5 - w_1w_2w_3v_4u_5 - u_1w_2v_3u_4w_5 \\
&\qquad = \sum \left[a\rho_1^+\rho_2^+\rho_3^+\eta_4\eta_5 + b\rho_1^-\rho_2^-\rho_3^-\eta_4\eta_5 + c\eta_1\eta_2\rho_3^+\rho_4^+\rho_5^+ + d\eta_1\eta_2\rho_3^-\rho_4^-\rho_5^- \right].
\end{aligned} \tag{5.15}$$

The second diagram gives the same identity with $\sigma_4^+ \leftrightarrow \sigma_4^-$, $\tau_4^+ \leftrightarrow \tau_4^-$, $\sigma_5^+ \leftrightarrow \sigma_5^-$, $\tau_5^+ \leftrightarrow \tau_5^-$. In either case, the loop 1245 is redundant, because when it is polarized, either 123 or 345 is polarized. Note that in the second diagram the loop 345 is not oriented and the last two contributions of (5.15) become proportional to the polarized loops $\rho_3^+\rho_4^-\rho_5^-$ and $\rho_3^-\rho_4^+\rho_5^+$.

Finally, we give a three-loop example, the box diagram equipped with diagonals. Let 1, 2, 3, 4 label the legs of the box and 5, 6 the diagonals. Define the leg orientations so that

the oriented loops are 1234, 125 and 236. Then the identity

$$z_1z_2z_3z_4z_5z_6 - u_1v_2z_3z_4z_5u_6 + u_1w_2v_3z_4v_5u_6 - u_1w_2w_3v_4v_5w_6 - z_1u_2v_3z_4v_5z_6 + z_1u_2w_3v_4v_5v_6$$
$$-v_1u_2w_3w_4w_5v_6 - z_1z_2u_3v_4z_5v_6 + v_1z_2u_3w_4u_5v_6 - w_1v_2u_3w_4u_5w_6 - v_1z_2z_3u_4u_5z_6$$
$$+w_1v_2z_3u_4u_5u_6 - w_1w_2v_3u_4w_5u_6 + v_1u_2v_3u_4w_5z_6 + u_1v_2u_3v_4z_5w_6 + w_1w_2w_3w_4w_5w_6 \sim 0,$$

holds, where the right-hand side of (3.9), which we do not report in full form, is a sum of polarized monomials. The polarized loops are 125, 236, 345 and 146, the last two being nonoriented.

6 Perturbative unitarity of quantum field theories

In this section we show how to use the algebraic cutting equations to prove the perturbative unitarity of quantum field theories. We begin with nonderivative scalar theories. For definiteness, we may consider the φ^4 theory, described by the Lagrangian

$$\mathcal{L} = \frac{1}{2}(\partial_\mu\varphi)(\partial^\mu\varphi) - \frac{m^2}{2}\varphi^2 - \frac{\lambda}{4!}\varphi^4,$$

which is renormalizable in $D \leqslant 4$. Alternatively, we may take the φ^6 theory, which is renormalizable in $D \leqslant 3$, or the φ^3 theory, which is renormalizable in $D \leqslant 6$. The discussion is actually independent of the form of the potential and the number of legs carried by the vertices, as long as they do not contain derivatives. Derivative vertices may be included with a few extra manipulations, which we describe at the end of this section. There, we also generalize the arguments to fields of different spins and nonrenormalizable theories.

Define the polar numbers

$$\sigma^\pm_{\mathbf{k}\epsilon} = \pm\frac{1}{2\omega_{\mathbf{k}\epsilon}}\frac{1}{k^0 \mp \omega_{\mathbf{k}\epsilon}}, \qquad \tau^\pm_{\mathbf{k}\epsilon} = -(\sigma^\mp_{\mathbf{k}\epsilon})^*, \tag{6.1}$$

where $\omega_{\mathbf{k}\epsilon} = \sqrt{\mathbf{k}^2 + m^2 - i\epsilon}$. The poles of $\sigma^+_{\mathbf{k}\epsilon}$, $\tau^+_{\mathbf{k}\epsilon}$ are located below the real axis and those of $\sigma^-_{\mathbf{k}\epsilon}$, $\tau^-_{\mathbf{k}\epsilon}$ are located above the real axis. The combinations

$$z_{\mathbf{k}\epsilon} = \sigma^+_{\mathbf{k}\epsilon} + \sigma^-_{\mathbf{k}\epsilon} = \frac{1}{k^2 - m^2 + i\epsilon}, \qquad w_{\mathbf{k}\epsilon} = -z^*_{\mathbf{k}\epsilon}, \qquad u_{\mathbf{k}\epsilon} = \sigma^+_{\mathbf{k}\epsilon} - (\sigma^+_{\mathbf{k}\epsilon})^*, \qquad v_{\mathbf{k}\epsilon} = \sigma^-_{\mathbf{k}\epsilon} - (\sigma^-_{\mathbf{k}\epsilon})^*,$$

give the propagators, their conjugates and the cut propagators. As before, we can use a different ϵ for each propagator.

Given a Feynman diagram G with V vertices and I internal legs, we assign loop energies and an orientation to it as specified by proposition 1 of section 2. We can promote the

energy assignments to assignments for the full momenta of the internal legs. So doing, we obtain a parametrization of G in momentum space.

The Feynman rules we have used so far are made of (3.3) plus the rule that an unmarked vertex is equal to $+1$ and a marked vertex is equal to -1. The Feynman rules commonly used in quantum field theory are slightly different, since they have an extra factor i for each propagator (cut or not) and an extra factor $-i\lambda$ for each vertex (marked or not), λ being the coupling:

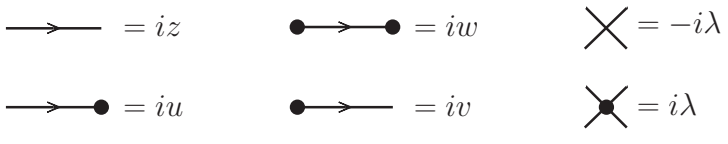

(6.2)

Each time we compute a diagram with the rules of the previous sections, we miss the overall factor $i^I(-i\lambda)^V$ with respect to the more common notation (6.2). For the rest of this section, we switch to (6.2).

After these redefinitions, the propagator iw connecting two marked points is the complex conjugate of the propagator iz connecting two unmarked points. Moreover, the propagators iu and iv connecting a marked point to an unmarked one are real. Finally, the marked vertices are the complex conjugates of the unmarked vertices.

Now we turn to the identity (3.9) and integrate it on the loop momenta. If G contains no tadpoles, the right-hand side vanishes, because it is a sum of polarized monomials. We recall that a polarized monomial has a polarized loop γ_{pol}. As explained in section 4, we can reparametrize the loop integral so that the energy e of γ_{pol} is one of the integrated variables. The integral on e is zero by the residue theorem, since its integrand has poles only above or below the real axis and we can close the integration path on the half plane that contains no poles. The integral of the left-hand side of (3.9) thus also vanishes, which gives the cutting equation. Once we multiply the identity by the factors $i^{I+V}(-\lambda)^V$ and switch to the notation (6.2), we arrive at the common diagrammatic cutting equation

$$G(p_1, \cdots, p_n) + \bar{G}(p_1, \cdots, p_n) = - \sum_{\text{proper markings } M} G_M(p_1, \cdots, p_n), \tag{6.3}$$

where $p_1, \cdots, p_n$ are the external momenta, G is the diagram with all unmarked vertices, $\bar{G}$ is the diagram with all marked vertices, and G_M denotes a diagram with a "proper" marking, i.e. with at least one marked vertex and one unmarked vertex.

Strictly speaking, (6.3) is the common cutting equation only in the limit $\epsilon \to 0$, where the cut propagators force the energy to flow from the unmarked endpoints to the marked endpoints. In that limit, numerous marked diagrams vanish due to energy conservation. Those which survive are precisely the usual cut diagrams. Nevertheless, it is always possible

to view a marked diagram as a cut diagram by means of closed cuts that circle subdiagrams made of marked vertices. This way, we can extend the common terminology by calling equation (6.3) a cutting equation even at $\epsilon \neq 0$.

There is a caveat, though: we know that the diagrams that contain tadpoles are not covered by the theorem of section 3. Thus, as far as we know now, equation (6.3) only holds for diagrams that contain no tadpoles. We can extend formula (6.3) to the whole set of diagrams as follows.

Tadpoles are loop diagrams with a unique vertex, $V = 1$, so they have as many internal lines as loops, by the topological identity $L - I + V = 1$. A three-loop example of a tadpole and a two-loop example of diagram with a tadpole are

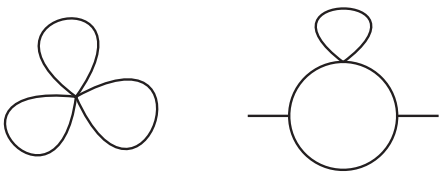

(6.4)

We recall that the reason why the diagrams with tadpoles are not covered by the theorem is that tadpoles lead to the integrals of single polar numbers, which are not convergent. Indeed, they behave as $\int \mathrm{d}k^0/k^0$ for k^0 large.

Tadpoles and diagrams with tadpoles can be straightforwardly included in the treatment, as long as they satisfy one additional assumption, which we call the *tadpole assumption*: the value of a tadpole with an unmarked vertex must be opposite to the value of its marked version. Graphically,

(6.5)

Now we show that the tadpole assumption allows us to derive the cutting equations satisfied by the diagrams that contain tadpoles. Consider such a diagram, and call it G_T. If we replace its tadpoles with external legs, we obtain a diagram $G_{\hat{T}}$ that satisfies (6.3).

For example, let G_T denote the second diagram of equation (6.4). If we replace the tadpole subdiagram with an external leg, we obtain a diagram $G_{\hat{T}}$ that is equivalent to the triangle diagram treated in the previous section:

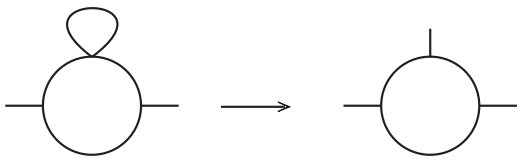

We know that $G_{\hat{T}}$ satisfies the identity obtained by equating the sum (5.10) to zero, which leads to formula (6.3). Now, take (5.10) and consider the upper-right external leg and the vertex ν to which it is attached. Suppress that leg and glue the tadpole to the vertex ν. Thanks to the first identity of equation (6.5), it does not matter whether ν is marked or not, since the value of the tadpole (neglecting the minus sign due to the marked vertex, because it is already counted inside $G_{\hat{T}}$) in the same in both cases. This means that the tadpole attachment amounts to multiplying the sum (5.10) by an overall factor. What we obtain by doing this and equating the total to zero is precisely the cutting equation satisfied by G_T.

The property illustrated in this simple example can be generalized to all tadpole diagrams G_T, as long as the tadpole assumption holds. Ultimately, to derive the cutting equations of tadpole diagrams, it is sufficient to ignore the tadpole subdiagrams and apply the procedure used for every other diagram.

It is easy to check that the scalar theories we are considering satisfy the tadpole assumption. For example, the value of the one-loop tadpole is [with the rules (6.2)]

$$\int \frac{\mathrm{d}^D k}{(2\pi)^D} \frac{i(-i\lambda)}{k^2 - m^2 + i\epsilon} = -i\lambda \frac{\Gamma\left(1 - \frac{D}{2}\right)}{(4\pi)^{D/2}} (m^2 - i\epsilon)^{(D-2)/2} \to -i\lambda \frac{\Gamma\left(1 - \frac{D}{2}\right)}{(4\pi)^{D/2}} m^{D-2}, \qquad (6.6)$$

while its marked version has the opposite value. The reason is that the marked version carries a minus sign due to the marked vertex and two other minus signs that compensate each other. Recall that the propagator connecting two marked points is $iw = -iz^*$. The conjugation of z flips the sign of the prescription $+i\epsilon$, which leads to a factor -1 that compensates the minus sign in front of iz^*. Thus, the first identity of (6.4) holds.

The L-loop tadpole is equal to the L-th power of (6.6), divided by $(-i\lambda)^{L-1}$. It satisfies the second identity of (6.4), because its marked version carries a minus sign for the marked vertex, while the minus signs coming from the relation $iw = -iz^*$ still compensate each other.

We have proved that, in the end, all Feynman diagrams satisfy the diagrammatic cutting equations (6.3). From this point on, the proof of perturbative unitarity can proceed according to the common strategy [4].

The proof extends to (local) theories with derivative vertices. The algebraic cutting equations are the same. The difference is that, before switching to the diagrammatic cutting equations, we must multiply both sides of formula (3.9) by appropriate polynomial numerators. We must show that the right-hand side still vanishes after integrating on the energies. This is less obvious than before.

When the numerator contains enough powers of the energy, contact terms may appear. Contact terms collapse propagators and generate new types of vertices and diagrams, which obey their own cutting equations. As shown in ref. [4], it is possible to associate each

diagram G with a set of separate cutting equations that involve no contact terms, the sum of which is equivalent to the G cutting equations at $\epsilon \to 0$. For this reason, there is no loss of generality in assuming that contact terms are absent. Since the propagators we are considering contain two powers of the energy in the denominators, we can assume that the numerators of the diagram G contain at most one power of each loop energy.

As before, we can restrict to diagrams G with no tadpoles, since tadpoles are easily attached to G at the end. Thus, every polarized loop $\gamma_{\rm pol}$ that appears in $\mathcal{P}_G$ contains two or more internal legs. If the internal legs are at least three, the energy integral is still convergent: each polar number behaves like $1/E$ for large energy E, while the numerator provides at most one E power; since the integrand of a polarized loop has all the poles on the same side of the integration path, the residue theorem gives zero.

The only case that deserves attention is when the polarized loop $\gamma_{\rm pol}$ has two legs, and, therefore, two vertices, which we call ν and ν'. We can assume that $\gamma_{\rm pol}$ is oriented. Due to the nontrivial numerator, we get the integrals

$$\frac{1}{4\omega_1\omega_2}\int_{-\infty}^{+\infty}\frac{\mathrm{d}E}{2\pi}\frac{E}{(E-\alpha\pm i\epsilon)(E-\beta\pm i\epsilon')} = \mp\frac{i}{8\omega_1\omega_2}, \tag{6.7}$$

depending on the polar numbers of $\gamma_{\rm pol}$, where α and β are real. We have not included the values of the vertices in formula (6.7). We want to show that the contributions (6.7) cancel each other. The reason is that each polarized loop that contributes with the upper sign, i.e. $\gamma_{\rm pol} = \sigma_1^+\sigma_2^+$, $\tau_1^+\sigma_2^+$, $\sigma_1^+\tau_2^+$, $\tau_1^+\tau_2^+$, is compensated by a polarized loop that contributes with the lower sign, i.e. $\gamma_{\rm pol} = \sigma_1^-\sigma_2^-$, $\tau_1^-\sigma_2^-$, $\sigma_1^-\tau_2^-$, $\tau_1^-\tau_2^-$.

Consider the left-hand side of equation (3.9). Isolate the contributions where $\gamma_{\rm pol} = \sigma_1^+\sigma_2^+$ and $\gamma_{\rm pol} = \sigma_1^-\sigma_2^-$. They come from the diagrams G_M where both ν and ν' are unmarked (recall that $\gamma_{\rm pol}$ is oriented) and the legs of the loop are $z_1 z_2$. Such diagrams compensate each other, because the coefficients of $\sigma_1^+\sigma_2^+$ and $\sigma_1^-\sigma_2^-$ are the same, but the values of the polarized loops are opposite, by formula (6.7). A similar argument applies to the pair $\tau_1^+\tau_2^+$ and $\tau_1^-\tau_2^-$, which comes from $w_1 w_2$ (with both ν and ν' marked), as well as the pair $\sigma_1^+\tau_2^+$ and $\tau_1^-\sigma_2^-$, which comes from $u_1 v_2$, and finally the pair $\tau_1^+\sigma_2^+$ and $\sigma_1^-\tau_2^-$, which comes from $v_1 u_2$. In the last two cases one vertex ν or ν' is marked and the other one is unmarked.

We conclude that the proof of perturbative unitarity based on the algebraic cutting equations applies to all scalar field theories, including those that have derivative vertices, as well as the nonrenormalizable ones. Following the guidelines of ref. [4], the proof can also be generalized to the theories that include fermions, gauge fields and gravity, as long as they are local, Hermitian and their kinetic terms are polynomials of degree two (in the case of bosons) or degree one (in the case of fermions) in the time derivatives.

7 Parity symmetry

Some transformations relate algebraic cutting equations that may look different, but are actually equivalent. Consider the polarity flipping, that is to say the exchanges

$$\sigma_i^+ \longleftrightarrow \sigma_i^-, \qquad \tau_i^+ \longleftrightarrow \tau_i^-. \tag{7.1}$$

At the level of the propagators, this operation leaves z_i and w_i invariant and exchanges u_i with v_i. By the Feynman rules (3.3), it is equivalent to flip the orientations of all the internal legs of the diagram G. We call (7.1) *parity* transformation.

In the case of one-loop diagrams, the right-hand side $\mathcal{P}_G$ of the identity (3.9) is invariant, by formula (3.11). Consequently, the left-hand side is also invariant. However, this fact may become apparent only after expanding it as a sum of polar monomials. Check for example the identity (5.9), associated with the triangle diagram.

When the number of loops exceeds one, both the left- and right-hand sides of (3.9) may change under the parity transformation. For example, it is easy to check that $\mathcal{P}_G$ does change in the case of the self-energies (3.8).

The diagrams G and $\bar{G}$ and so the left-hand side of the diagrammatic cutting equation (6.3) are invariant. For this reason, (7.1) is a symmetry of the diagrammatic cutting equations. Nevertheless, the right-hand side of (6.3) may get organized differently after the transformation.

The algebraic cutting equations likely possess other hidden symmetries that are awaiting to be uncovered. For example, the parity transformation (7.1) can be performed on just one or more legs, instead of all of them. Moreover, the cut and uncut propagators are in some sense dual to each other, because both are linear combinations of half propagators and their different roles only emerge at the graphical level.

8 Conclusions

We have proved a set of polynomial identities for polar complex numbers, which provide a clearer understanding of perturbative unitarity in quantum field theory. To conclude, we make some remarks on the virtues of the algebraic approach to perturbative unitarity, in comparison with the usual approach.

Normally [1, 2, 3, 4], the cutting equations (6.3) are obtained by first proving the largest time equation in coordinate space and then taking its Fourier transform. The algebraic approach, on the other hand, allows us to jump directly to formula (6.3) in momentum space.

When tadpoles are absent, equation (6.3) holds for arbitrary positive values of the widths ϵ of the propagators (6.1). In particular, the widths ϵ need not be infinitesimal. If we choose a different ϵ for each internal leg, our algebraic theorem allows us to keep track of them efficiently throughout the calculation. Each propagator (cut or not) keeps its own ϵ from the beginning to the end and no mixing between the ϵs of different propagators does occur. This means that we are allowed to freely send them to zero in the order we want. When we do it, the cut propagators become those we are accustomed to, i.e.

$$\lim_{\epsilon\to 0} iu_{\mathbf{k}\epsilon} = (2\pi)\theta(k^0)\delta(k^2 - m^2), \qquad \lim_{\epsilon\to 0} iv_{\mathbf{k}\epsilon} = (2\pi)\theta(-k^0)\delta(k^2 - m^2).$$

Yet, we stress again that the identity (6.3) also holds when the cut propagators are $iu_{\mathbf{k}\epsilon}$ and $iv_{\mathbf{k}\epsilon}$, where ϵ is arbitrary, at least when tadpoles are absent. When tadpoles are present, the widths can be arbitrary everywhere but in the tadpoles, where they must be set to zero to ensure that the tadpole assumption holds.

If we do not use the algebraic theorem of this paper and make rather natural operations on the integrands, it is easy to generate inconvenient mixings between the ϵs of different propagators and encounter ill-defined distributions such as [5]

$$\frac{1}{\omega - \omega' - p^0 - i(\epsilon_1 - \epsilon_2)}, \tag{8.1}$$

where $\omega = \sqrt{\mathbf{k}^2 + m_1^2}$ and $\omega' = \sqrt{(\mathbf{k} - \mathbf{p})^2 + m_2^2}$ are some frequencies, p is an external momentum and k is a loop momentum. It is possible to show (see ref. [5] for details) that the ill-defined part of (8.1) ultimately does not contribute. The theorem proved here guides us through the calculations without ever meeting these ill-defined distributions.

Going through the analysis recently made in ref. [4], where the assumptions behind the proof of perturbative unitarity have been relaxed to a minimum, it is possible to realize that the properties just emphasized can also be proved in the usual nonalgebraic approach. However, an approach like the algebraic one, which makes them so apparent, is of great advantage.

The usual approach is also responsible for giving some false impressions. For example, it suggests that the cut propagators must force the energy propagation in a given direction. This is not true, as the validity of (6.3) at nonvanishing widths points out. Again, it is not impossible to show this fact in the usual approach, because the assumption about the energy flow enters the proof only at a later stage [4]. However, the roles of the various ingredients of the proof become much clearer when the algebraic cutting equations are used.

Acknowledgments

We are grateful to U. Aglietti and M. Piva for useful discussions.

References

[1] R.E. Cutkosky, Singularities and discontinuities of Feynman amplitudes, J. Math. Phys. 1 (1960) 429;

M. Veltman, Unitarity and causality in a renormalizable field theory with unstable particles, Physica 29 (1963) 186.

[2] G. 't Hooft, Renormalization of massless Yang-Mills fields, Nucl. Phys. B 33 (1971) 173;

G. 't Hooft, Renormalizable Lagrangians for massive Yang-Mills fields, Nucl. Phys. B 35 (1971) 167.

[3] C. Becchi, A. Rouet and R. Stora, The Abelian Higgs Kibble model, unitarity of the S-operator, Phys. Lett. B 52 (1974) 344;

C. Becchi, A. Rouet and R. Stora, Renormalization of gauge theories, Ann. Phys. (NY) 98 (1976) 287;

G. Curci and R. Ferrari, An alternative approach to the proof of unitarity for gauge theories, Nuovo Cimento A 35 (1976) 273;

T. Kugo and I. Ojima, Local covariant operator formalism of non-Abelian gauge theories and quark confinement problem, Prog. Theor. Phys. Suppl. 66 (1979) 1;

C. Becchi, "Lectures on the renormalization of gauge theories," in Les Houches 1983, Proceedings, Relativity, Groups and Topology, II, p. 787.

[4] D. Anselmi, Aspects of perturbative unitarity, Phys. Rev. D 94 (2016) 025028, 16A1 Renormalization.com and arXiv:1606.06348 [hep-th].

[5] D. Anselmi and M. Piva, to appear.